
# Final Technical report on physical modeling of effects of potential borrow areas on local wave transformation and beach processes

Prepared for

NYS DOS

Prepared by

Robert Wilson, Yicheng Huang and Henry Bokuniewicz
School of Marine and Atmospheric Sciences
Stony Brook University
Stony Brook, NY 11794-5000

**June 2018**

## Stony Brook University's COAST Institute


The Coastal Ocean Action Strategies (COAST) Institute was created in 1989 within the School of Marine and Atmospheric Sciences to assist in coastal zone management and coastal marine policy analysis. We do this by exploring future scenarios for Long Island's coastline and coastal environment and by working with policy makers and environmental managers in identifying and analyzing strategies that will conserve and, when necessary, rehabilitate the coastal ocean; by ensuring that not only is the best technical information included in developing the strategies, but economic and other critical information as well; and by forming effective linkages among environmental groups, the scientific community, lawmakers, regulators, and managers to tackle coastal environmental issues.

COAST has been called upon to assist in resolving coastal problems at home on Long Island, throughout the U.S. and in many parts of the world. COAST also provides a real world, action-learning laboratory for graduate students at MSRC. Each year students who are interested in coastal management and policy take part in gathering and analyzing data, in transforming data into information, and in synthesizing information-all targeted at identifying and evaluating management alternatives to attack the problems that COAST is helping to solve.

## *Introduction*

Marine sand on the Outer Continental Shelf is a resource potentially available to New York for coastal restoration, and beach nourishment. To examine the potential impacts of sand extraction offshore, we have conducted modeling of select wave climates based on wave and wind characteristics, bottom bathymetry, and shoreline orientation. This technical report describes progress on a sensitivity analysis to identify and prioritize use of sand borrow areas which may result in minimal impacts to the physical system. Our work focuses specifically on three potential borrow areas identified by BOEM; detailed surveys were done at Fire Island Inlet, Fire Island, and Moriches Inlet (**Figure 1**). Within each of these areas, potential and proven sand reserves were delineated by Flood et al. (2018; **Figure 2**)

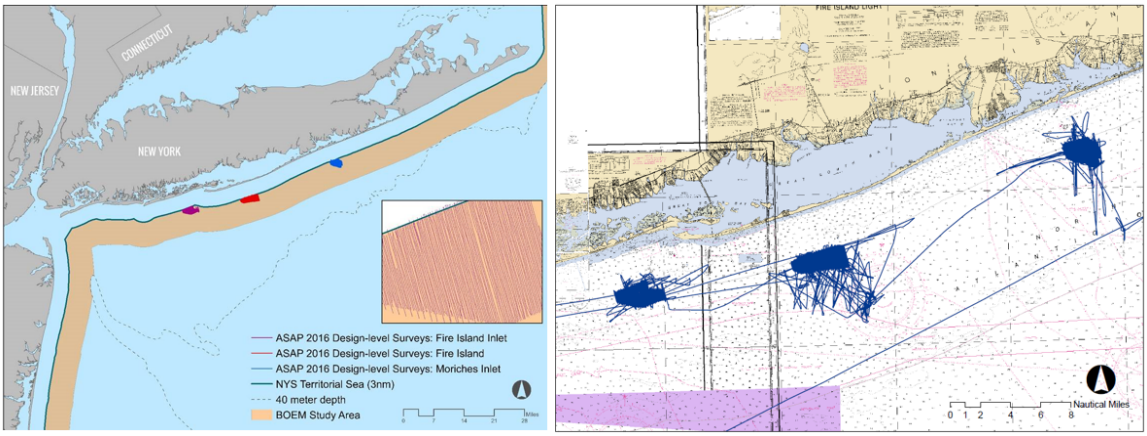


**Figure 1. Potential borrow areas identified by BOEM and geophysical survey tracks (BOEM Phase 2, 2016).**

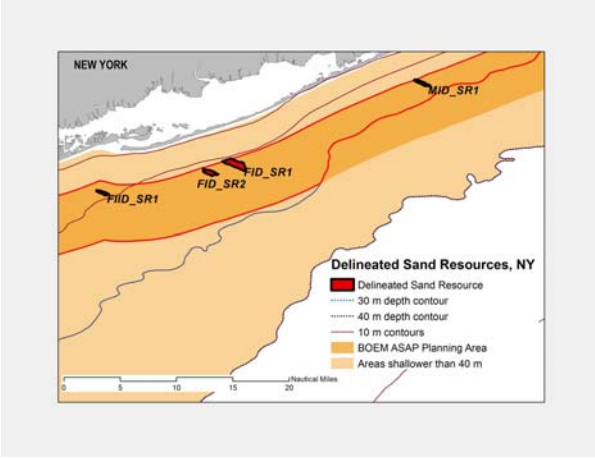


**Figure 2. Potential and proven designated sand reserves (Flood et al. 2016).**

## *Background*

An engineering study conducted by Benedet et al. (2013) examined effects of nearshore dredge borrows on volume changes in adjacent beaches by applying a morphological model Delft3D to idealized shore-parallel bathymetry. The sediment transport module of Delft3D integrates the effects of waves, currents, sediment transport on morphological development. Benedet et al. examined a range of parameters, including seabed cross-shore geomorphology (sea bed slope), local wave climate, sediment supply, and borrow area characteristics (e.g. distance offshore, depth of cut, cross-shore and alongshore extents). They examined response to single-wave condition characterized by significant wave height, period and angle of approach, and to an annual wave climate for which these wave properties varied seasonally. It should be emphasized that results presented here are long-term annual statistical forecasts. Important basic findings included:

- The depth of the cut and the cross-shore length of the borrow areas greatly influenced the magnitude of the impact on the adjacent beach volume change.
- The distance of the borrow areas from the shore influenced the magnitude and location of the impacts because of the oblique wave incidence.
- An inverse relationship between water depth where the borrow area was located and the magnitude of its impacts on adjacent beach volume change.
- Depth of cut had pronounced effects in shallow water, but in water depths greater than 8 m, depths of cut did not significantly affect impact on adjacent beaches. NY State defines "Structural Hazard Areas", for example, as sections of the shore where the long-term rate of shoreline recession is greater than one foot per year. Changes in shoreline recession rate greater than one foot per year could be considered significant.

Similar studies in other areas have shown impacts are site specific. In some cases, the shoreline accretes, the lee of the borrow site accretes while in others erosion develops either directly behind the borrow site or off to the side. Borrow areas in deep water or sufficiently far from shore had minimal impacts. A wave transformation modeling study by Dalyander et al. (2015) was used to assess the effects of proposed offshore borrow areas on the nearshore wave field. Effects were assessed over a range of wave conditions and were gaged by changes in significant wave height and wave direction inshore of the borrow sites, as well as by changes in the estimated longshore sediment transport rate.

The Phase I analysis by Wilson et al. (2016) relied on numerical wave transformation modeling similar to that employed by Dalyander et al. (2015). In the analysis we concluded that the effects of idealized borrow areas on significant wave height, $H_s$, and on wave direction, $\alpha$, are localized in vicinity of the area. Even long period swell tends to break well inshore of the modeled borrow area location which is three nautical miles offshore. Simulations did point to some possible divergence in volumetric transport inshore of the borrow area based on a conservative energy threshold of 0.01 $W/m^2$ at the initiation of wave

breaking to define the wave height, $H_b$, and angle of wave attack, $\alpha_b$, respectively at breaking. A less conservative threshold would imply a reduction in transport divergence. It should be emphasized that these were limited model simulations associated with single-wave condition characterized by specific significant wave height, wave period and angle of approach. To estimate the net effect of the offshore wave field on the shoreline over the course of a year, a full suite of realized waves for which wave properties varied seasonally should be taken into account, including representative extreme events.

## *Objectives*

Overall objectives of this physical wave modeling work are to assess the effects of potential sediment borrow areas on: a) nearshore wave climate and b) long-shore sediment transport, rate; c) divergence from that long-shore transport rate and d) shoreline recession. Specific objectives of this study include an assessment of these effects as posed by three potential borrow sites identified by BOEM (**Figure 1**). This study is not limited to these sites but they are the current focus.

## *Methods*

To meet study objectives, we followed aspects of the basic wave transformation methodology outlined in Dalyander et al. (2015). We have, however:

1. Expanded the model domain to give us capability to examine borrow areas not only off Fire Island but also borrow areas in vicinity of both the eastern and western ends of the Fire Island;
2. Updated model bathymetry, especially in vicinity of the potential BOEM borrow areas located in **Figure 1** to incorporate the most contemporary observations;
3. Substantially increased the inventory of wave and wind forcing scenarios beyond those applied during Phase I. This includes forcing with wave properties which vary spatially along the open boundary, and;
4. Developed an assessment of the effects of borrow areas on longshore transport and transport divergence associated with more complete forcing scenarios, including complete excavation of proven and potential sand reserves (**Figure 2**).

## *Expanded model domain*

**Figure 3** shows the model domain expanded eastward to Block Island as well as to the south along the New Jersey coast. The figure also shows an unstructured grid for this expanded domain developed using SMS gridding software (www.aquaveo.com) which supports the SWAN wave model. The grid resolution varies from approximately about 1000 m in the off-shore region to approximately 10 m in the near-shore region. Minimum grid resolution in vicinity of a borrow area is approximately 10 m. Bathymetry shown in **Figure 3** is updated NOAA bathymetry interpolated to the grid as discussed below. **Figure 4** shows an example of grid refinement applied when simulating the effects of a particular borrow area, in this case the Fire Island borrow area.

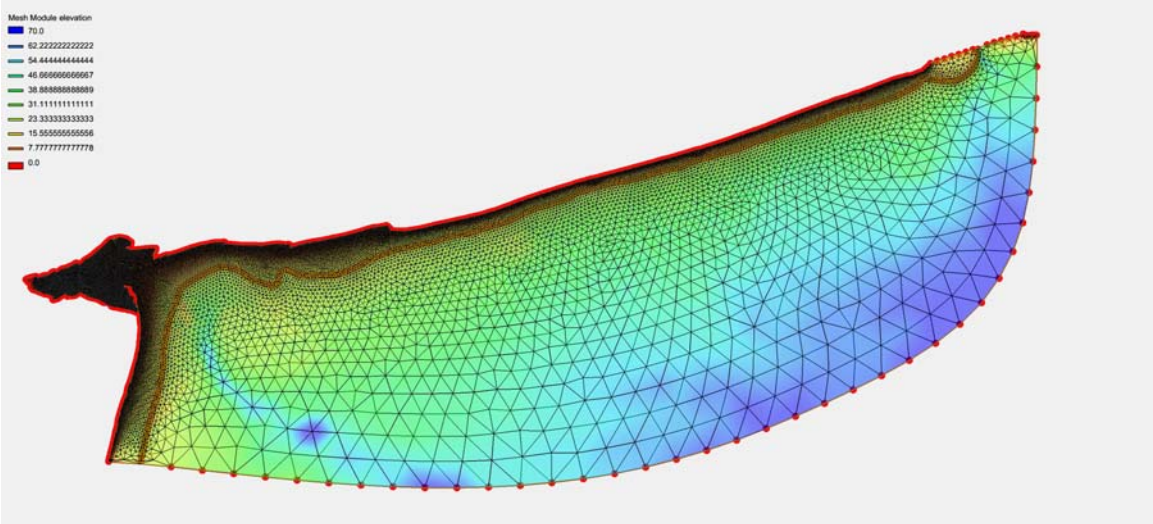


**Figure 3. Wave model domain and unstructured grid and bathymetry.**

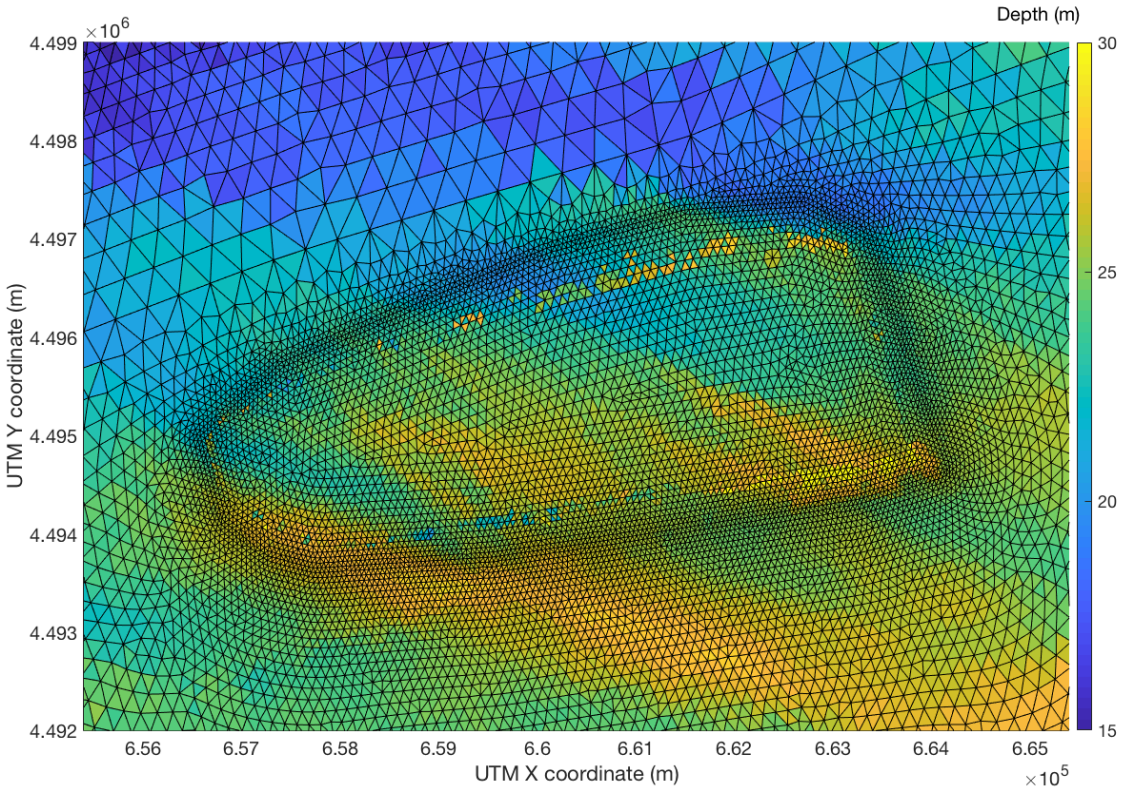


**Figure 4. Grid refinement in vicinity of Fire Island borrow area.**

## *Expanded model bathymetry*

All bathymetry data used in Phase I simulations was NOAA US Coastal Relief data (www.ngdc.noaa.gov/mgg/coastal/grddas01/grddas01.htm). Data from this site has the major advantage than datums associated with different surveys have been reconciled. They have the disadvantage that some of the contributing survey data sets are extremely old. Model bathymetry shown in Figures 2 and 3 has been developed from a composite (**Figure 5**) of NOAA data sets (www.ngdc.noaa.gov ) most of which are dated 1990-2016 and none of which are older than 1975.

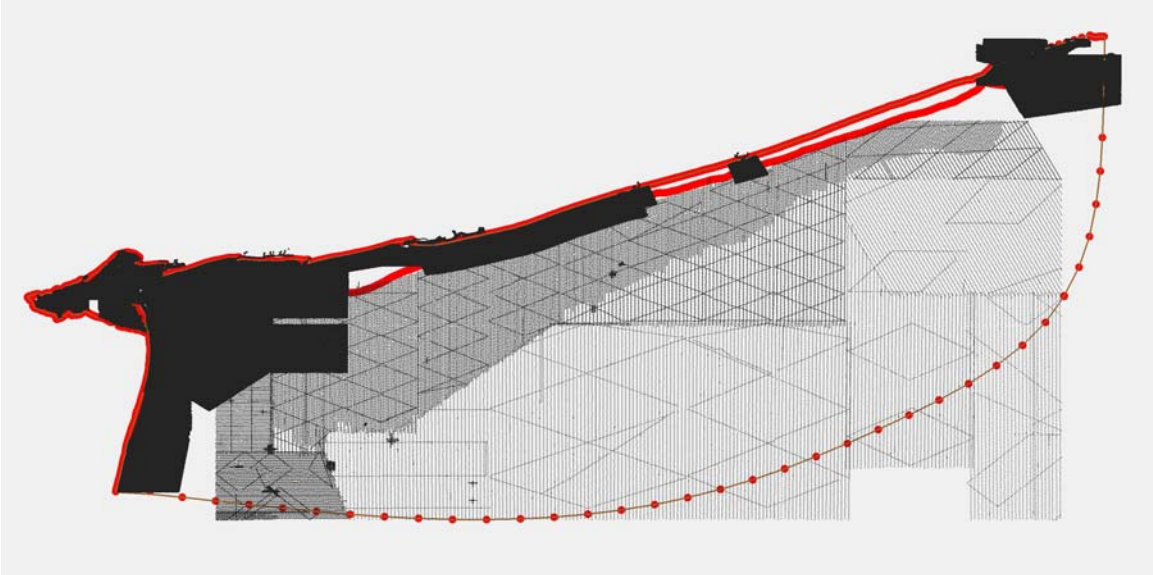

**Figure 5. NOAA survey data sets (www.ngdc.noaa.gov ) used to update model bathymetry.**

## *Defining wave and wind forcing scenarios*

The offshore wave climate on the open boundary applied as model forcing is developed from both long-term records from regional wave buoys (www.ndbc.noaa.gov/ ) 44025, 44017, 44065 and 44097 (www.ndbc.noaa.gov/ ) (**Figure 6**), and from archived east coast WaveWatch III output (http://wis.usace.army.mil/hindcasts.html). Unlike the limited boundary forcing applied during Phase I, Phase II forcing accounts for wave properties (Hs, $\alpha$, and period) varying spatially along the open boundary.

The methodology for defining boundary forcing from buoy and WaveWatch III data developed by Dalyander et al. (2015) and Long et al. (2014) was refined in this present study as described below. Because LST is not linearly related to wave height, rather than using basic wave climate statistics (**Figure 6**), we used a longshore sand transport (LST) fraction statistic (**Figure 7**) to define boundary wave characteristics (direction $\theta$, significant wave height $S_H$, and period T). This statistic was defined as the fraction of LST associated with a

given (θ, $S_H$, T) bin divided by the total LST occurring over all bins. This statistic was developed from preliminary SWAN simulations used to estimate a mean wave breaking depth. Snell's law was applied to the wave climate time series at the buoy site (44025) to calculate the refracted significant wave height and wave direction at the mean wave breaking depth. This provided θ and $S_H$ at the wave breaking point. Relations (1) and (2) (Longuet-Higgins, 1952, 1972; defined below under ***Long-shore sand transport and transport divergence***) were then used to calculate the LST time series for a given bin and thereby the LST fraction statistic defined by:

$$f(Hs_i, \theta_i) = \frac{\sum_{(Hs(t_j),\theta(t_j)\in Bin_i} LST(t_j)}{\sum_{j=1}^{N} LST(t_j)}$$

It was this statistic that was used to define model forcing bins (θ, $S_H$, T) rather than basic wave climatology (**Figure 6**). In **Figure 7** positive and negative sand fractions relate to westward and eastward directed LST, respectively.

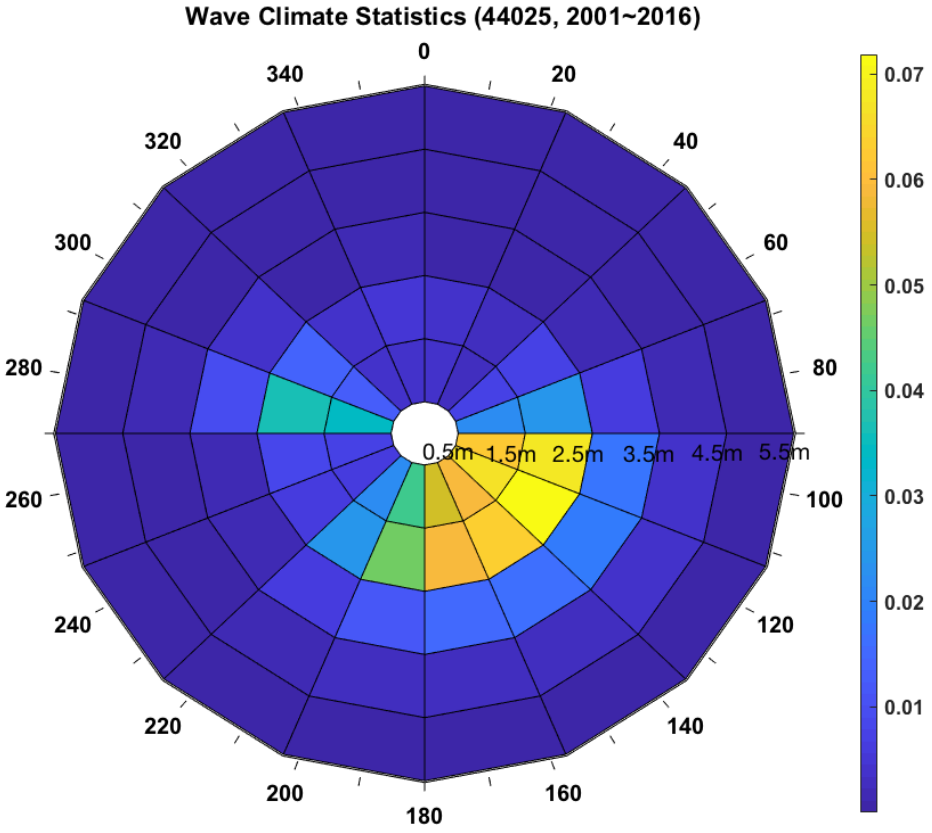


**Figure 6. Wave climate statistics (θ, $S_H$) derived from NOAA buoy 44025.**

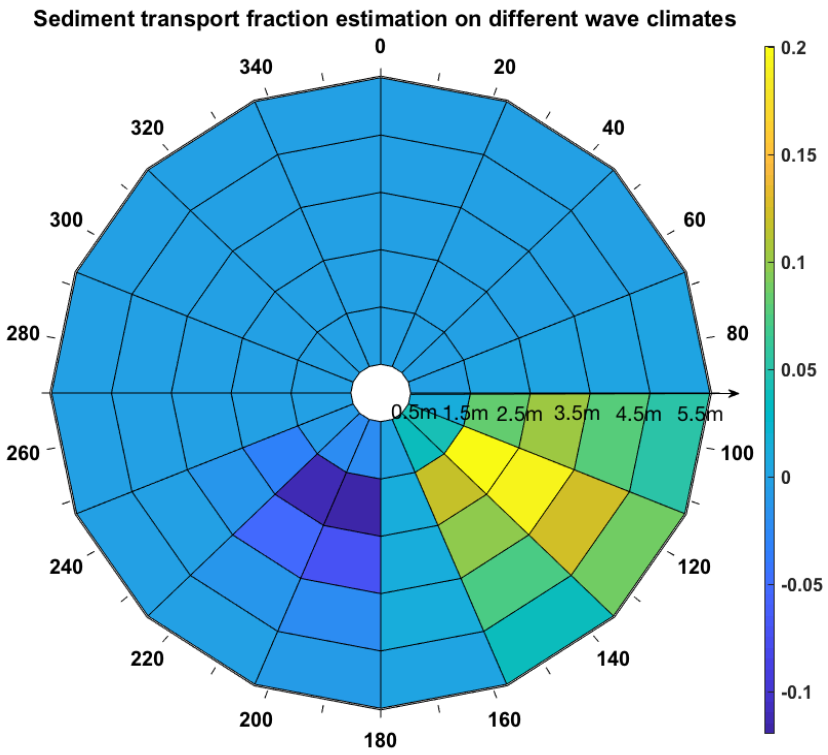


**Figure 7. LST fraction statistic used to define SWAN model forcing (see text).**

For the dominant wave bins defined in **Figure 7**, open boundary and local wind forcing data were extracted from archived WWIII data as outlined in the flow diagram in **Figure 8**.

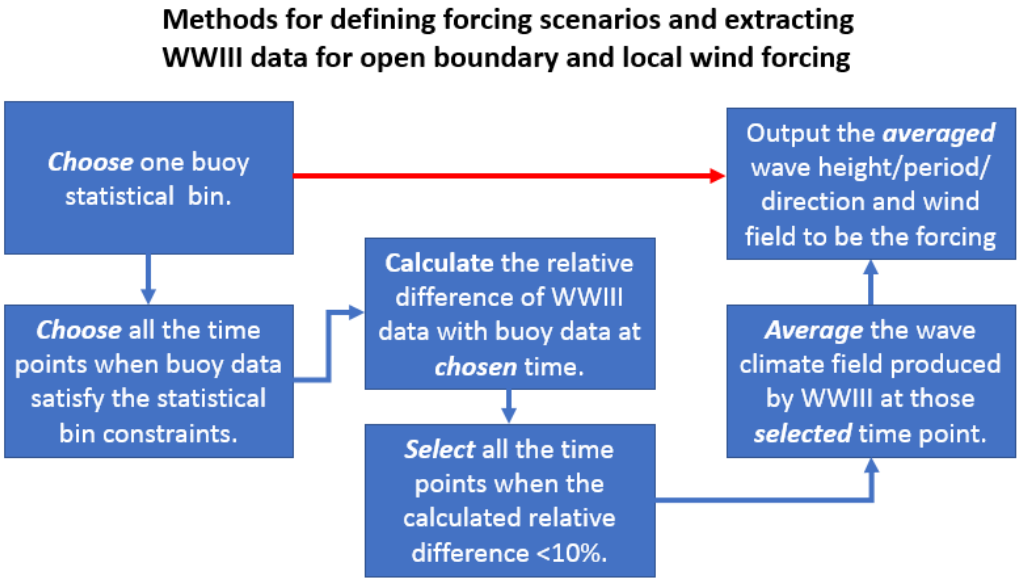


**Figure 8. Flow diagram describing extraction of WWIII data for open boundary and local wind forcing.**

Examples of open boundary ($\theta$, $S_H$, T) forcing for a bin centered on $\theta$ =123.25° are shown in **Figures 9-11**.

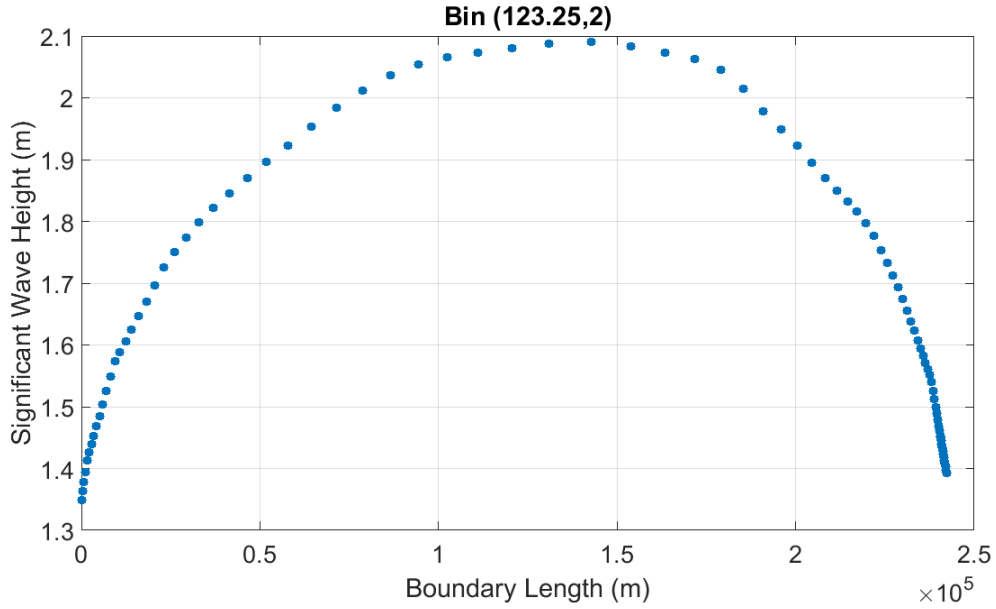


**Figure 9. Open boundary $S_H$ for bin (123.25,2) (see Figure 7).**

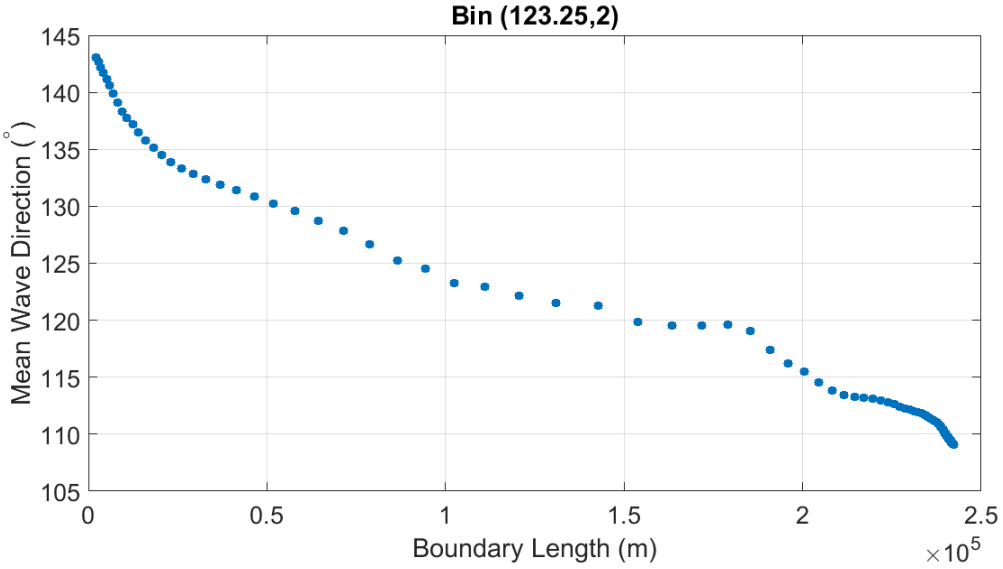


**Figure 10. Open boundary $\theta$ for bin (123.25,2) (see Figure 7).**

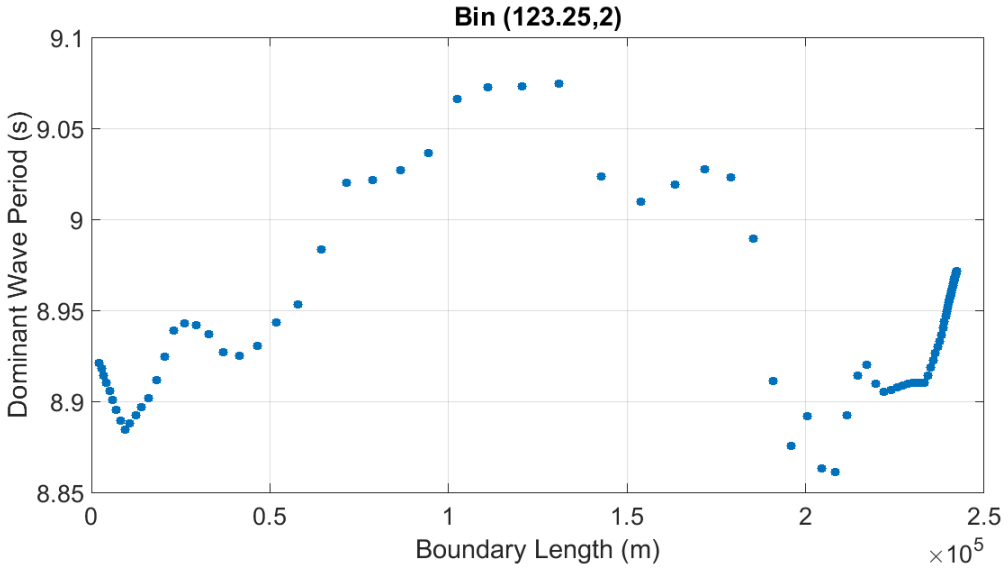


**Figure 11. Open boundary T for bin (123.25,2) (see Figure 7).**

## *Refraction patterns for FI borrow area for dominant wave forcing bins*

**Figures 12-15** show examples of the effects of borrow areas on wave refraction patterns for two dominant forcing bins identified in **Figure 7**: (123.25°,2) and (191.25°,2). This is presented as contours of anomalies in $S_H$ and θ which emphasize the magnitude and spatial extent of the borrow area effects. What is shown are relatively "significant" anomalies concentrated immediately inshore of the borrow area, and detectable anomalies over a coastline distance of up to 35 km. For forcing bin (123.25°,2) anomalies are skewed towards the west; for bin (191.25°,2) they are skewed slightly towards the east.

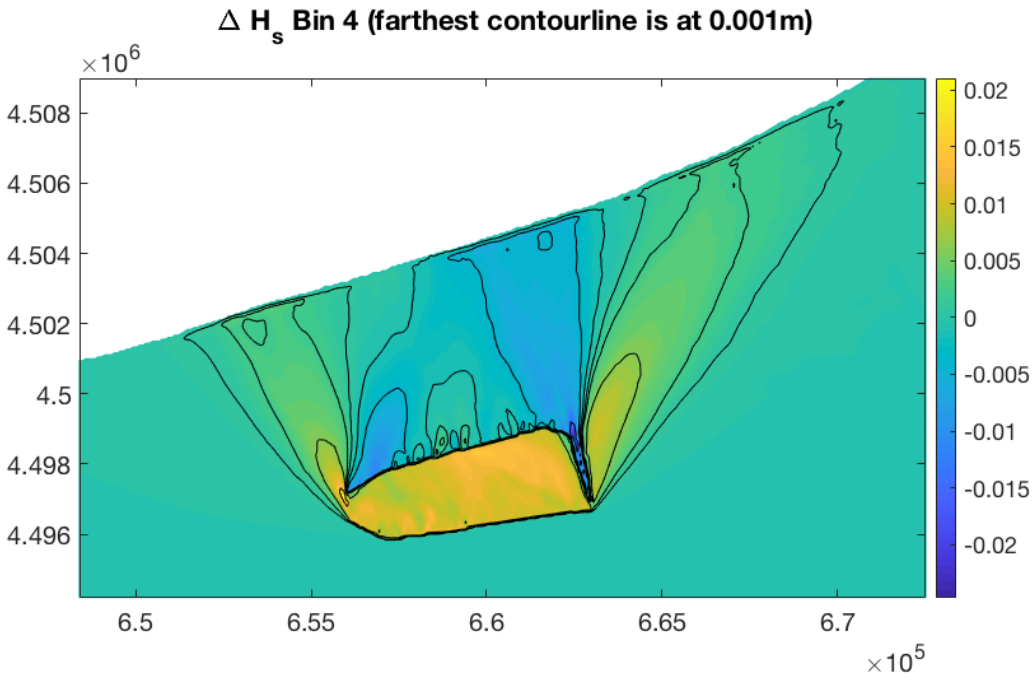


**Figure 12. $\Delta S_H$ for forcing bin (191.25,2) (see Figure 7).**

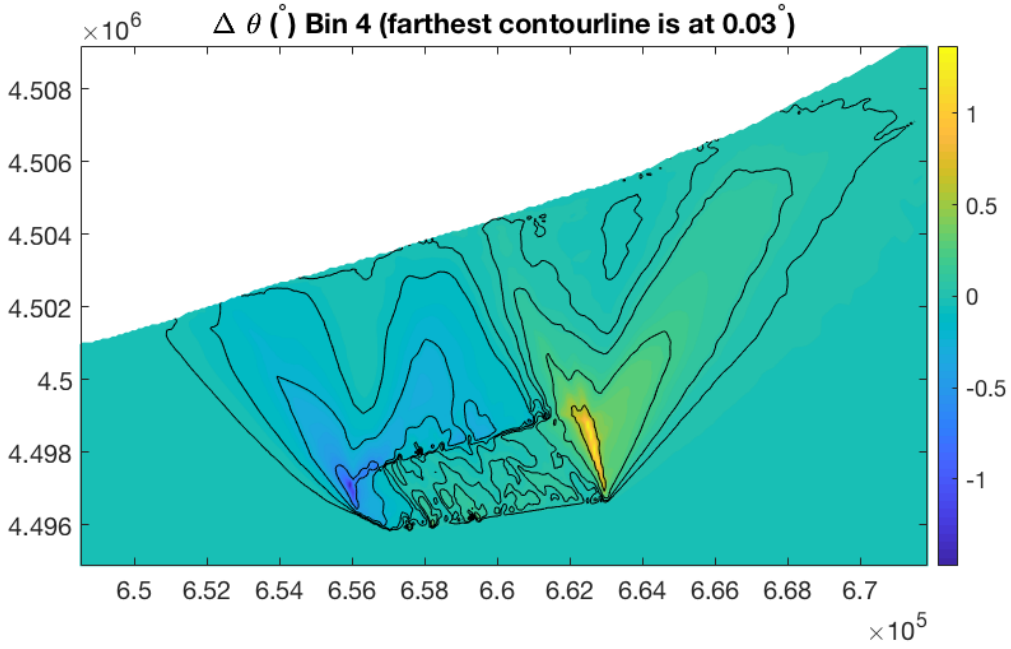


**Figure 13. $\Delta\theta$ for forcing bin (191.25,2) (see Figure 7).**

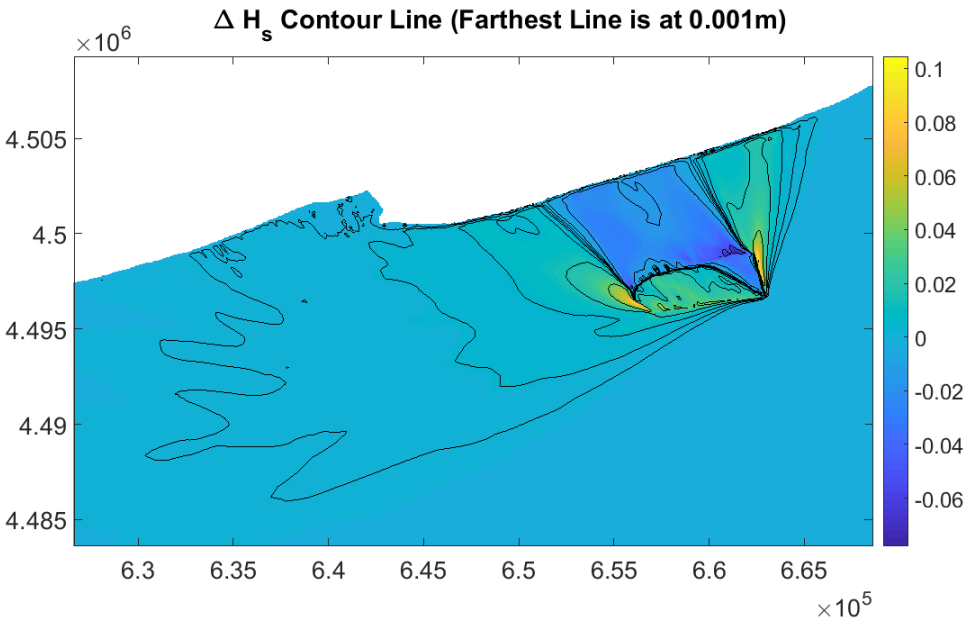


**Figure 14. $\Delta S_H$ for forcing bin (123.25,2) (see Figure 7).**

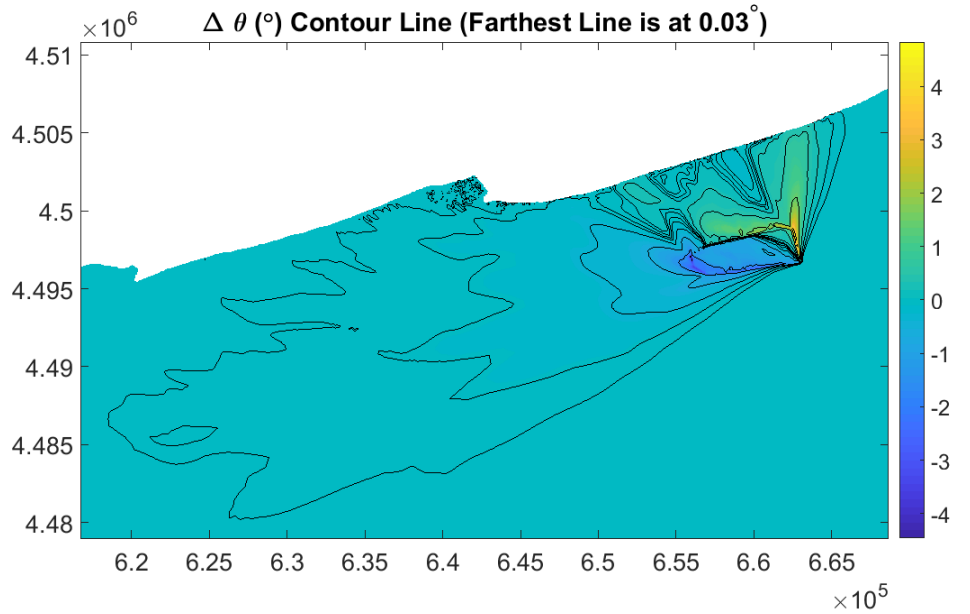


**Figure 15. $\Delta\theta$ for forcing bin (123.25,2) (see Figure 7).**

### *Long-shore sand transport, transport divergence, and shoreline change*

Long-shore volumetric sand transport $Q_l$ and its divergence is estimated following Dalyander et al. (2015) as:

$$Q_l = \frac{KP_l}{(\rho_s - \rho_w)g(1-n)} \qquad (1)$$

where $\rho_s$ ($2.65\times10^3$ kgm$^{-3}$) and $\rho_w$ ($1.024\times10^3$ kgm$^{-3}$) are the densities of sand and water and $n$ is sediment porosity (0.4). The empirical coefficient K was taken to be 0.8 by Dalyander et al. (2015), but other investigators have used values ranging from 0.25 to 0.77. Later, we will adopt a value of 0.25 based on a comparison of calculated values of LST with measurements.

$P_l$ is the longshore component of wave energy flux given by (Dean and Dalrymple, 2002):

$$P_l = 0.0884\rho_w g^{3/2} H_b^{5/2} \sin\alpha_b \cos\alpha_b \qquad (2)$$

where $H_b$ is breaking wave height approximated by Hs/1.4, and $\alpha_b$ is incident breaking wave angle relative to the shoreline.

**Figure 16** shows the longshore distribution of cross-shore transects used to obtain an estimate of LST produced by the dominant bins defined in **Figure 7**. It is important to understand that these are not the high resolution transects used to evaluate the effects of borrow areas on LST and its divergence. Results shown in **Figure 17** emphasize that the total LST produced by the 6 most dominant bins is directed towards the west and is of the same order as that inferred from limited beach survey data (Bokuniewicz, 2018). The LST associated with bin 4 (191.25°,2) alone (**Figure 18**) is directed towards the east with magnitude increasing towards the east. From this comparison, it is clear that bin 1 (123.25°,2) forcing is dominating the LST.

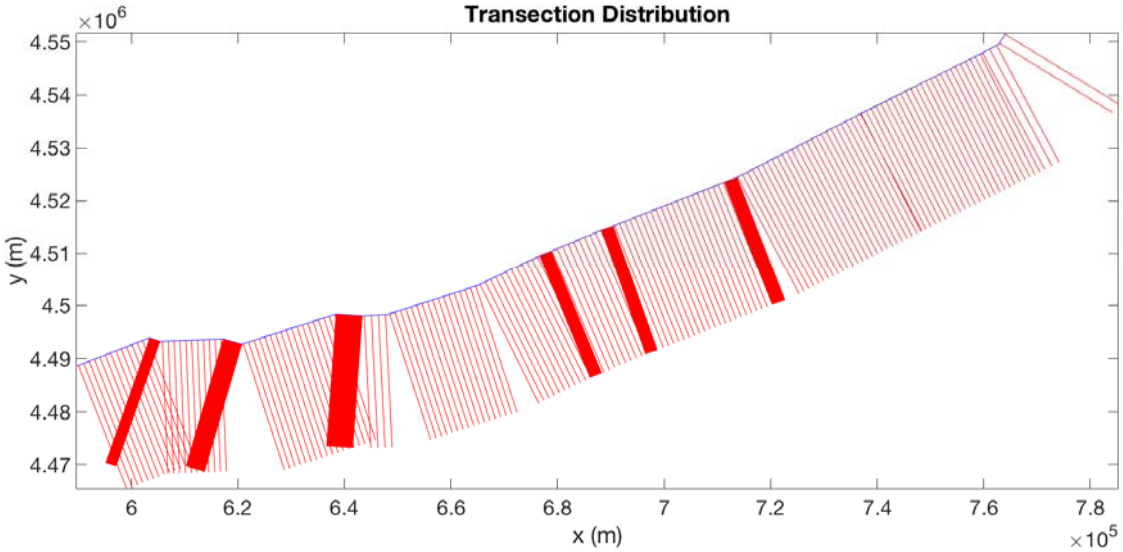


**Figure 16. Longshore distribution of transects used to estimate LST.**

Effects of borrow areas on longshore transport and its divergence were evaluated using high resolution transects in vicinity of the borrow area (**Figure 4**). Results for bin 1 (123.25°,2) and bin 4 (191.25°,2) forcing are presented separately in **Figures 19-20** and Figures **21-22**, respectively to emphasize the effects of wave direction. These results emphasize the longshore extent and magnitude of LST changes associated with a borrow area. Changes in longshore divergence in LST can also be related directly to possible beach recession.

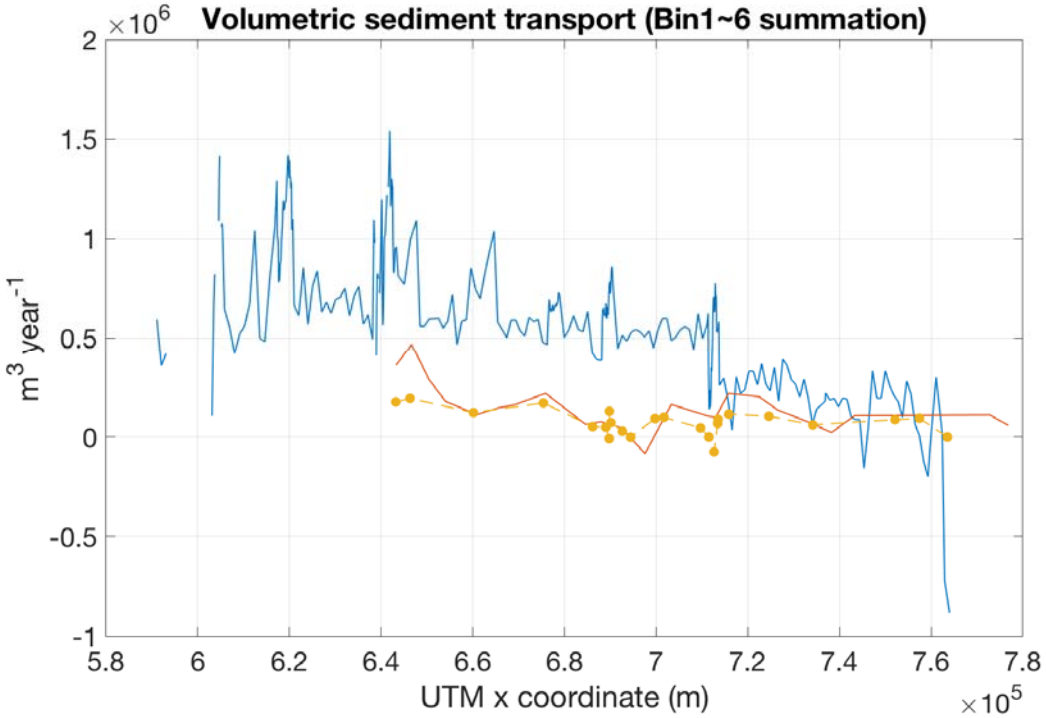


**Figure 17. Total LST (blue line) produced by wave forcing (see text); LST inferred from survey data (red lines).**

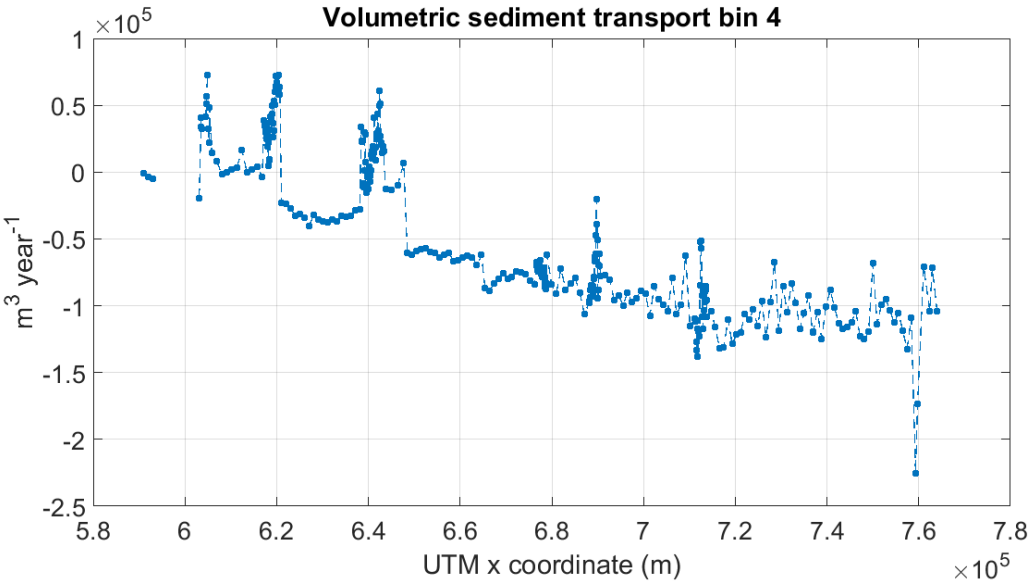

Figure 18. LST produced by bin 4 (191.25°,2) forcing alone.

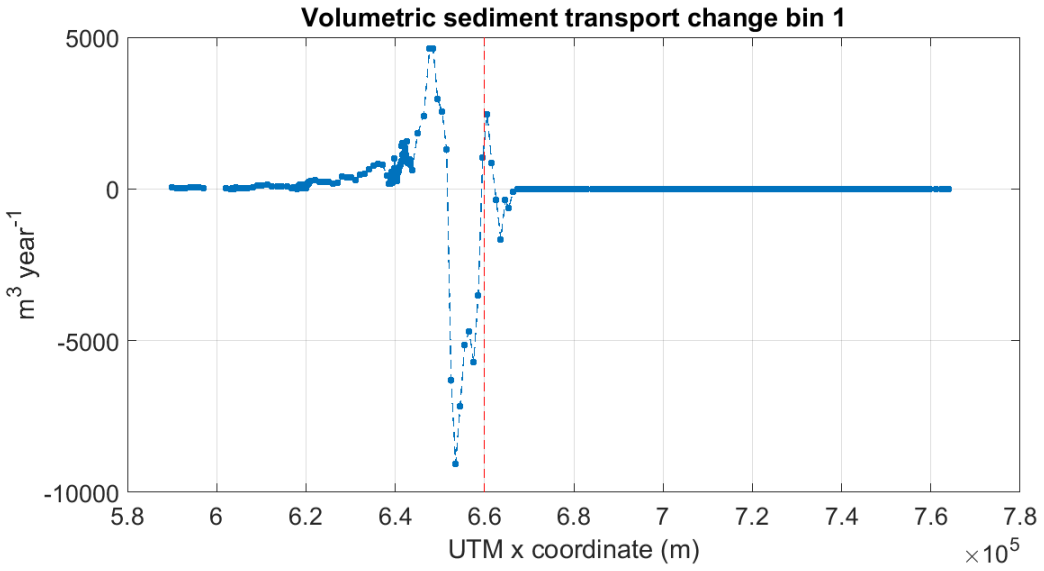


Figure 19. ΔLST associated with bin 1 (123.25°,2) forcing.

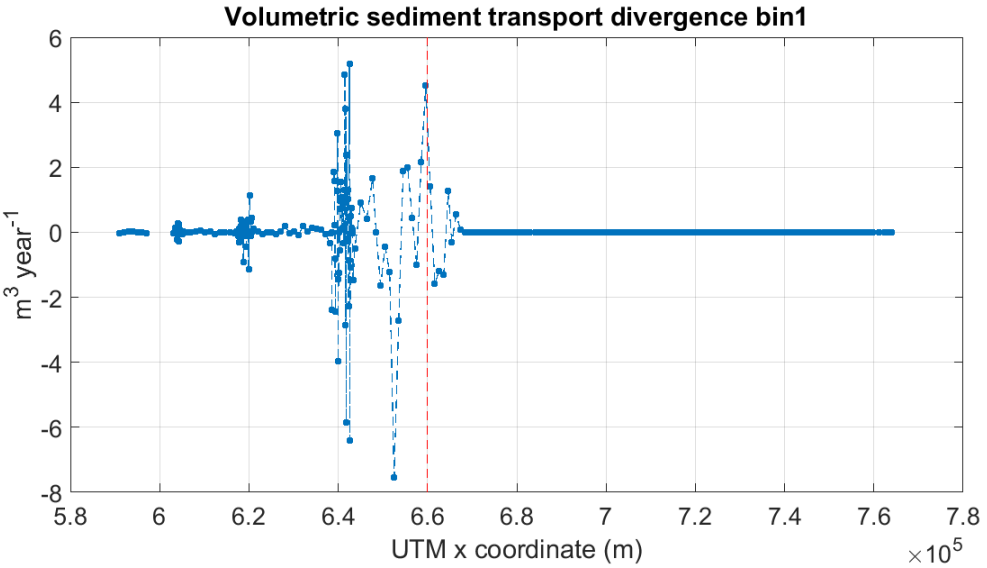


Figure 20. Change in LST divergence associated with bin 1 (123.25°,2) forcing.

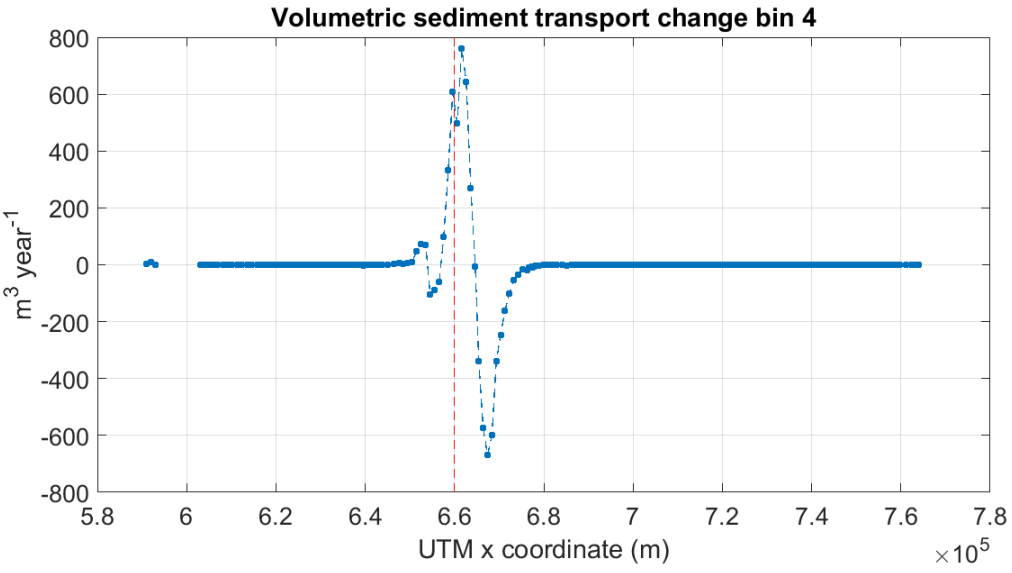


**Figure 21. ΔLST associated with bin 4 (191.25°,2) forcing.**

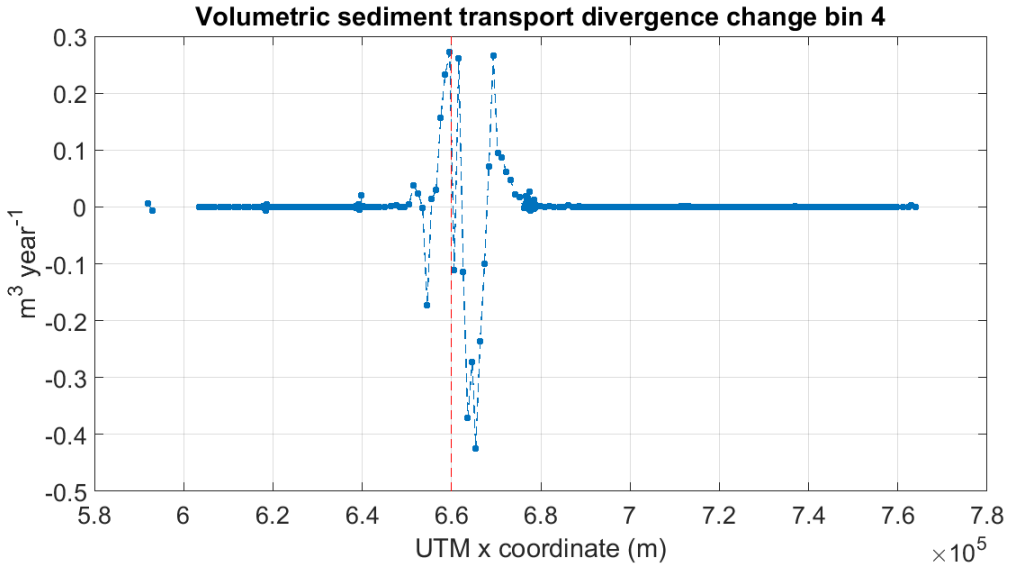


**Figure 22. Change in LST divergence associated with bin 4 (191.25°,2) forcing.**

The divergence in LST was used to estimate the advance or recession of the shoreline by applying a standard engineering expedient (Waldner, 2004). If more sand is leaving a stretch of beach at one end than is coming in at the other, the beach must erode to supply the difference. The oft-used expedient is used to estimate how much the shoreline will erode if the stretch of beach is losing sand or how much wider the beach will become if you add sand. This is expressed as "one cubic yard per foot per foot", that is, it takes one cubic yard of sand to change the shoreline position by one foot for every foot of shoreline length.

### *Results for seasonal wave forcing for the borrow areas and sub-areas*

Twenty-two bins representing wave conditions were used to calculate LST (**Figure 23**). Each was weighted according to the fraction of the year the particular wave condition was observed. In all, they represented 90.07% of the total LST.

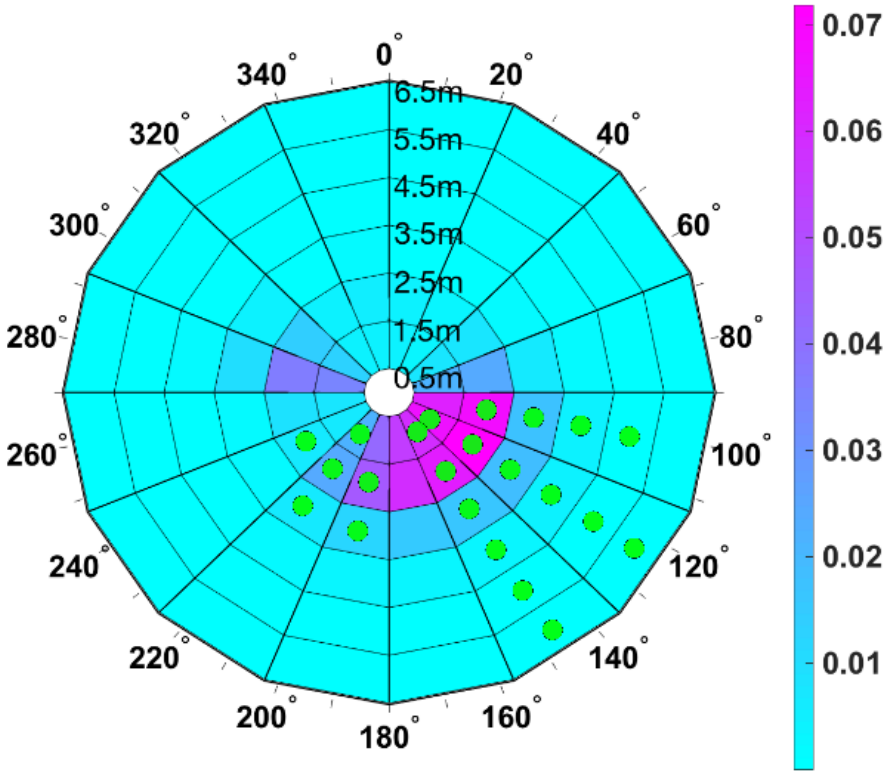


**Figure 23. The 22 wave condition bins used to calculate the total LST.**

Previous investigators have estimated LST from Fire Island Inlet to Montauk Point (Along the south shore of Long Island (Rosati et al. 1999; Kana 1995). The calculation of LST depends on the use of an empirical constant K. Previous applications have used values for this constant ranging from 0.25 to 0.8 (K=0.25 from Inman and Frautschy [1966], K=0.77 from Komar and Inman [1970], K=0.8 from Dalyander et al. [2016]). Comparisons between our calculations of LST and available regional field observations indicated that a value for the empirical coefficient of approximately 0.25 was appropriate (**Figure 24**). This lower value for K is consistent with analyses of observation by van Rijn (2014).

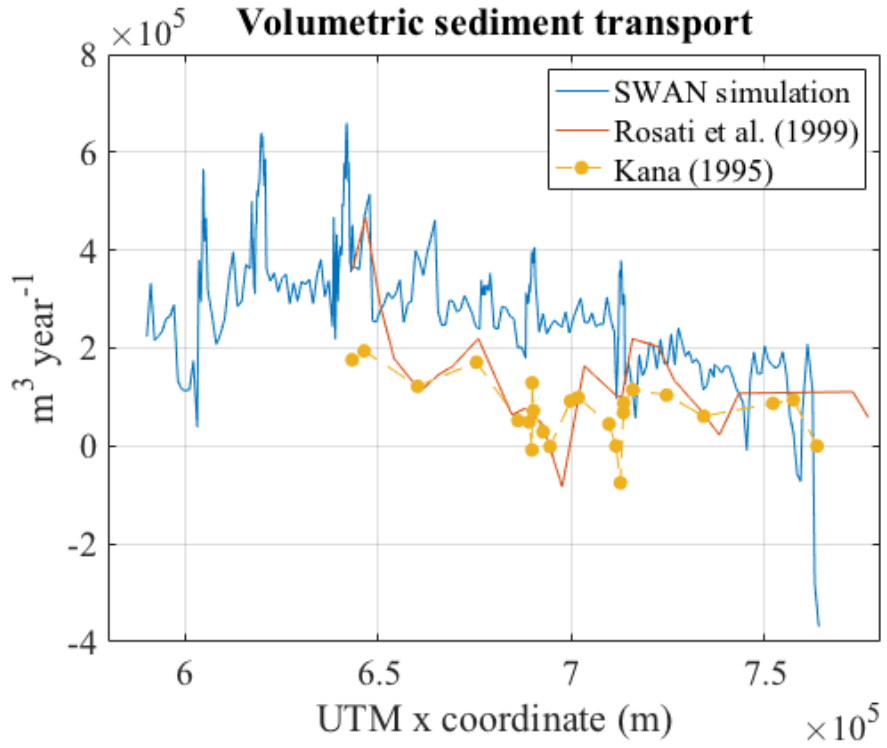


**Figure 24. Comparisons of calculated LST with available field observations of LST which imply an empirical coefficient K of 0.25.**

The presentation of the modeling results will be made all along New York's ocean shoreline from Breezy Point (Coney Island) to Montauk Point (**Figure 25**). For each of the three areas of detailed BOEM borrow-area surveys (**Figure 1**), LST was calculated first assuming that the entire surveyed borrow area was excavated to a depth of 4 meters. Positive values of LST indicated westward transport. The LST was then recalculated in each borrow area assuming that only the proven or potential sand reserves (**Figure 2**) were removed. Each LST scenario was compared to the LST calculated on the existing bathymetry. A change in LST was calculated as the LST after the hypothetical excavation minus the current, undisturbed LST. The divergence of LST and the change in divergence of LST was calculated for all cases and the engineering expedient of "one cubic yard per foot per foot" was applied to estimate change in shoreline retreat or advance.

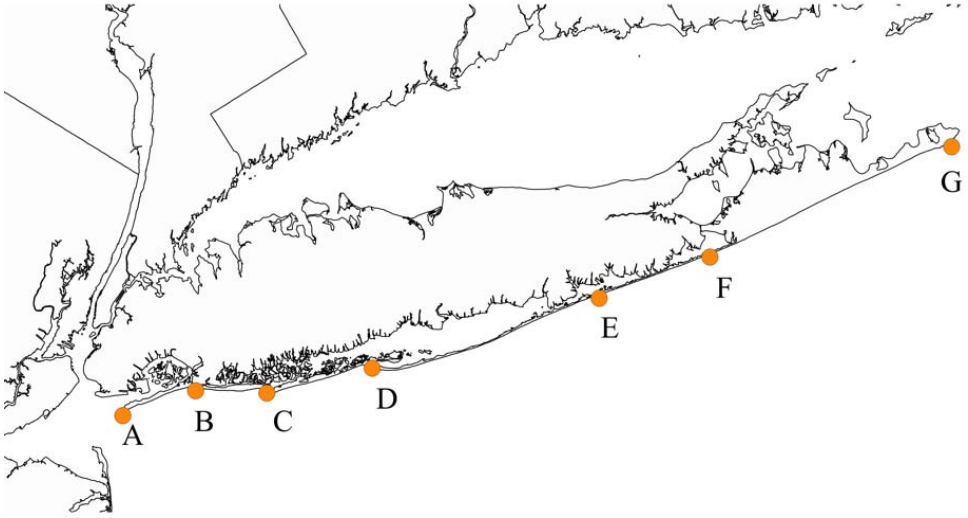


**Figure 25. Inlets positions referenced in Figures 26 -37.**

**Figures 26, 27 and 28** show the change in LST due to the excavation of the entire area covered by each detailed survey of the three borrow areas to a depth of 4 meters. In each case the LST was increased directly seaward on the borrow area, but flanked on each side by stretches of beach where the LST was decreased after excavation. The disturbed regions spanned about 30 km. Once these changes are effected by offshore sand mining in the borrow areas, they would be permanent, at least until the borrow area morphology is changed.

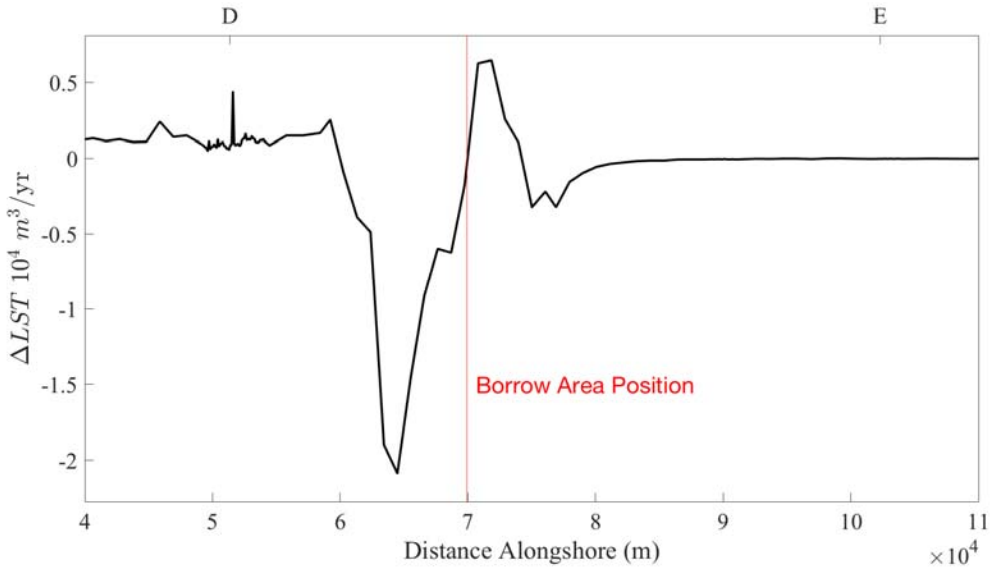


**Figure 26. The change in LST (LST after excavation minus the LST before excavation) due to the excavation of the entire area associated with the FI borrow area to a depth of 4 meters.**

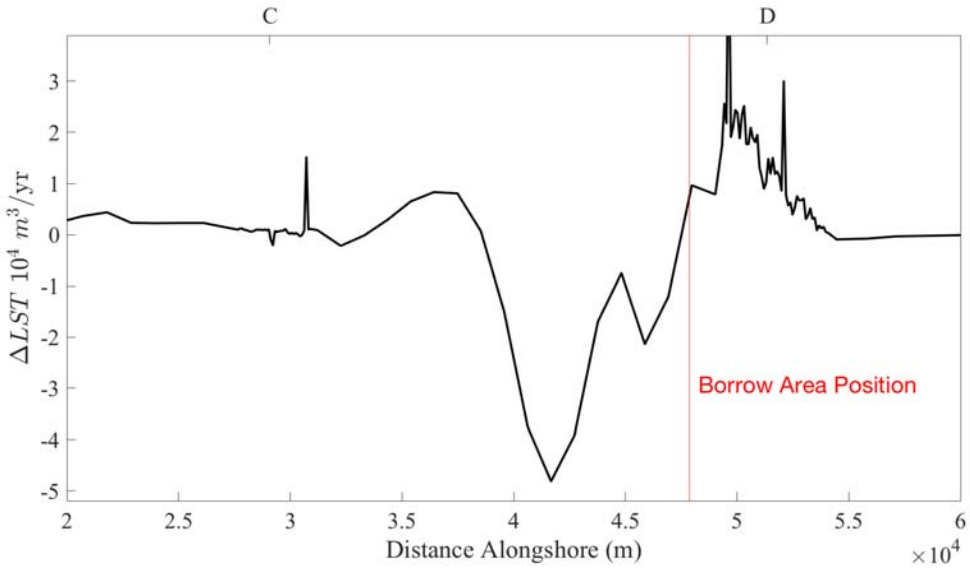


**Figure 27. The change in LST (LST after excavation minus the LST before excavation) due to the excavation of the entire area associated with the FI Inlet borrow area to a depth of 4 meters.**

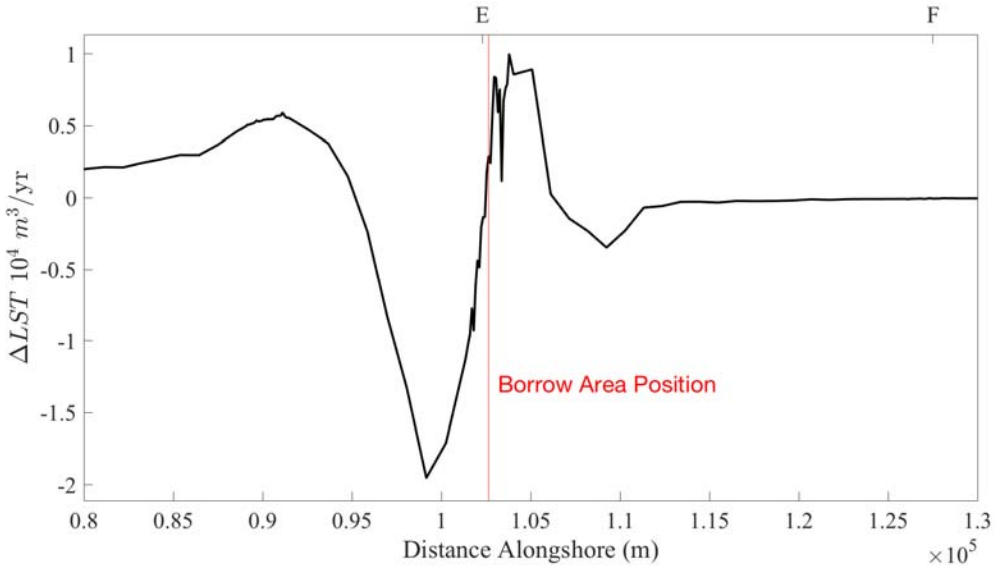


**Figure 28. The change in LST (LST after excavation minus the LST before excavation) due to the excavation of the entire area associated with the Moriches Inlet borrow area to a depth of 4 meters.**

The changes in LST after removal of only the identified potential and proven sand reserves identified by Flood et al. (2018) are shown in **Figures 29, 30 and 31**. The pattern of disturbance tended to show decreased LST immediately to the west of the excavated area flanked on either side by smaller increases in LST. The disturbed regions spanned about 15 km in the alongshore direction. Once these changes are effected by offshore sand mining in the borrow areas, they would be permanent, at least until the borrow area morphology is changed.

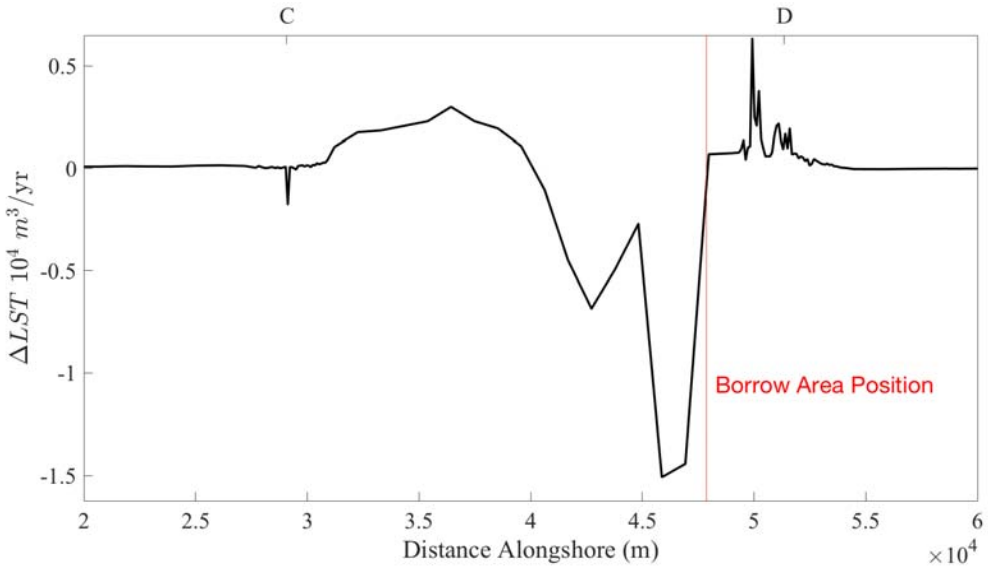


**Figure 29a. The change in LST (LST after excavation minus the LST before excavation) due to the excavation of potential sand reserves identified at the Fire Island Inlet site (Figure 29b).**

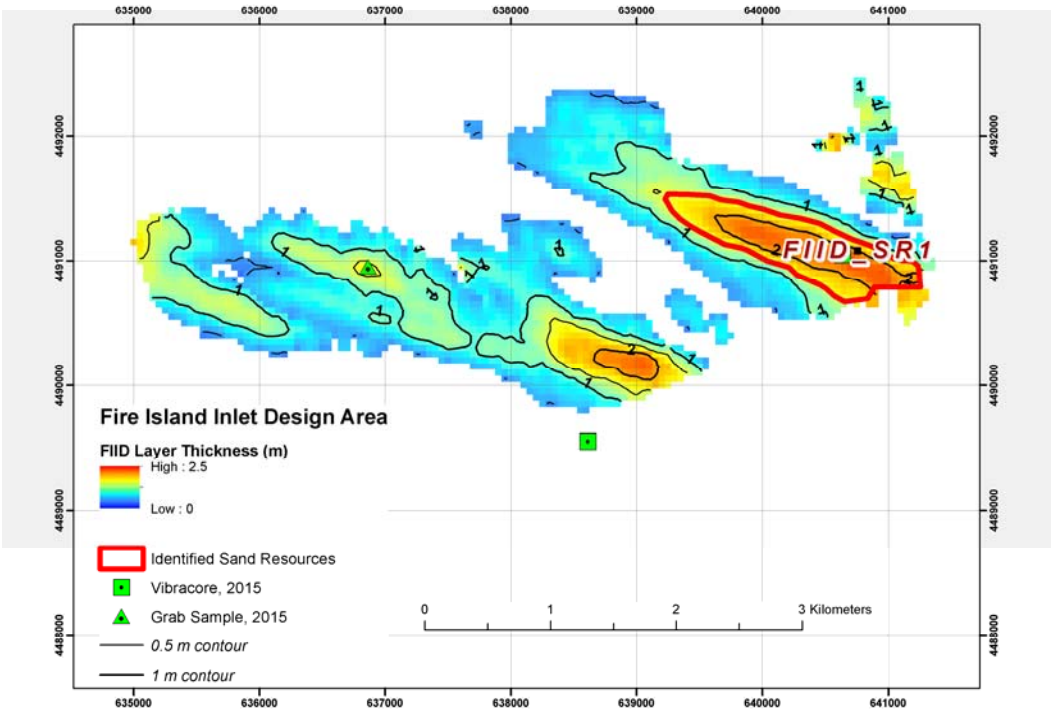


**Figure 29b. Potential and proven sand reserves identified at the Fire Island Inlet site by identified by Flood et al. (2018).**

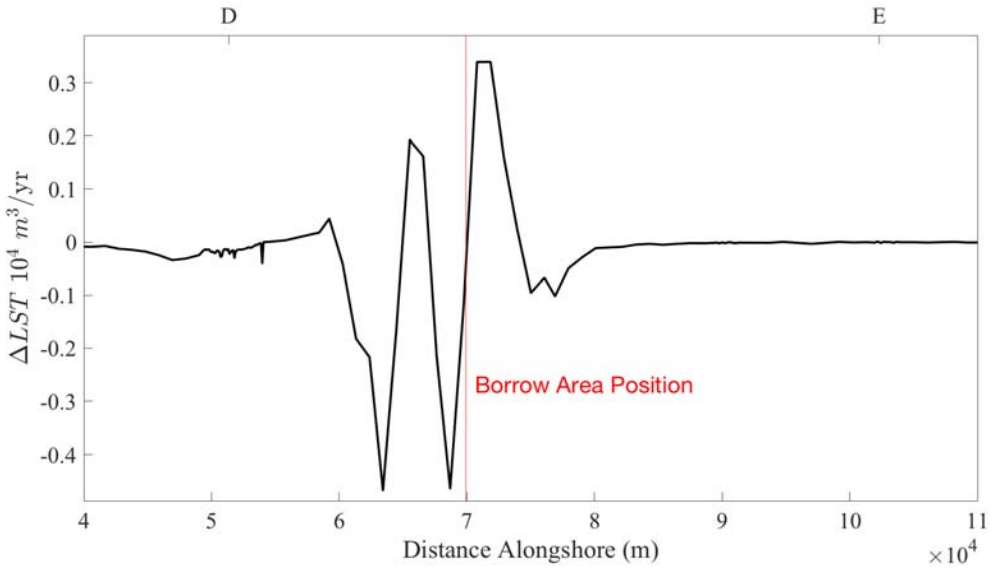


**Figure 30a. The change in LST (LST after excavation minus the LST before excavation) due to the excavation of potential sand reserves identified at the Fire Island site (Figure 30b).**

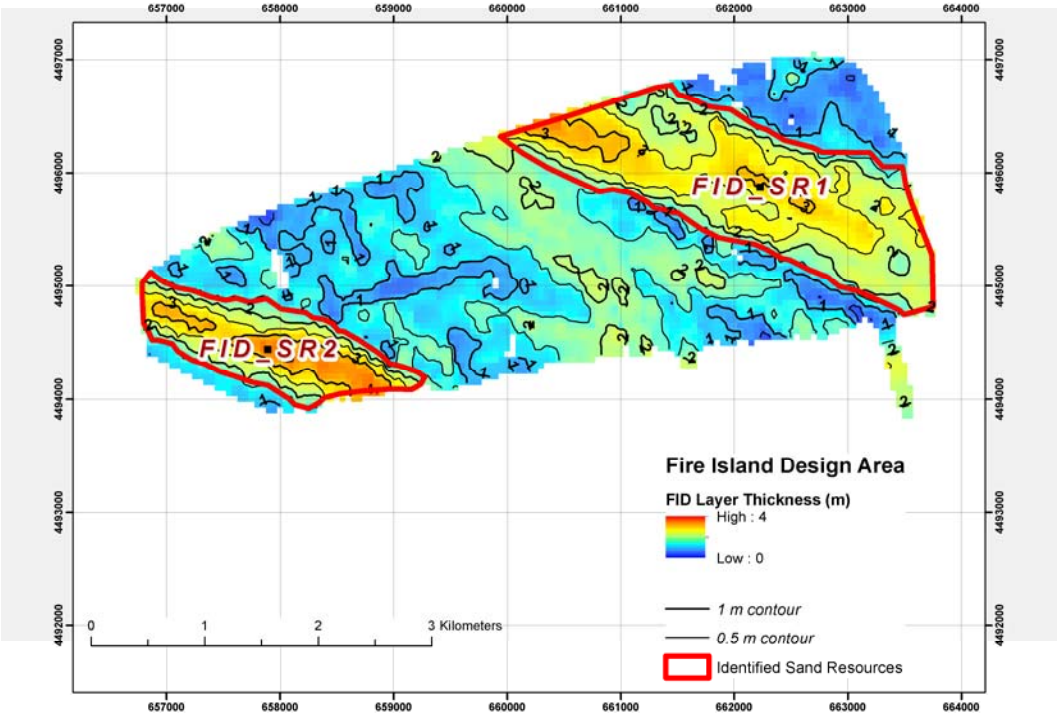


**Figure 30b. Potential and proven sand reserves identified at the Fire Island site by identified by Flood et al. (2018).**

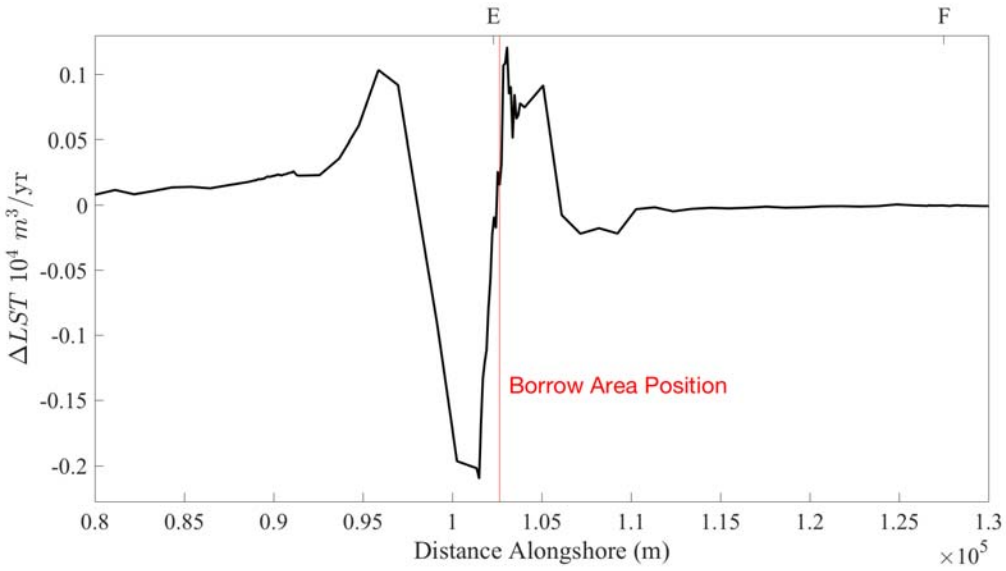


**Figure 31a. The change in LST (LST after excavation minus the LST before excavation) due to the excavation of potential sand reserves identified at the Moriches Inlet site (Figure 31b).**

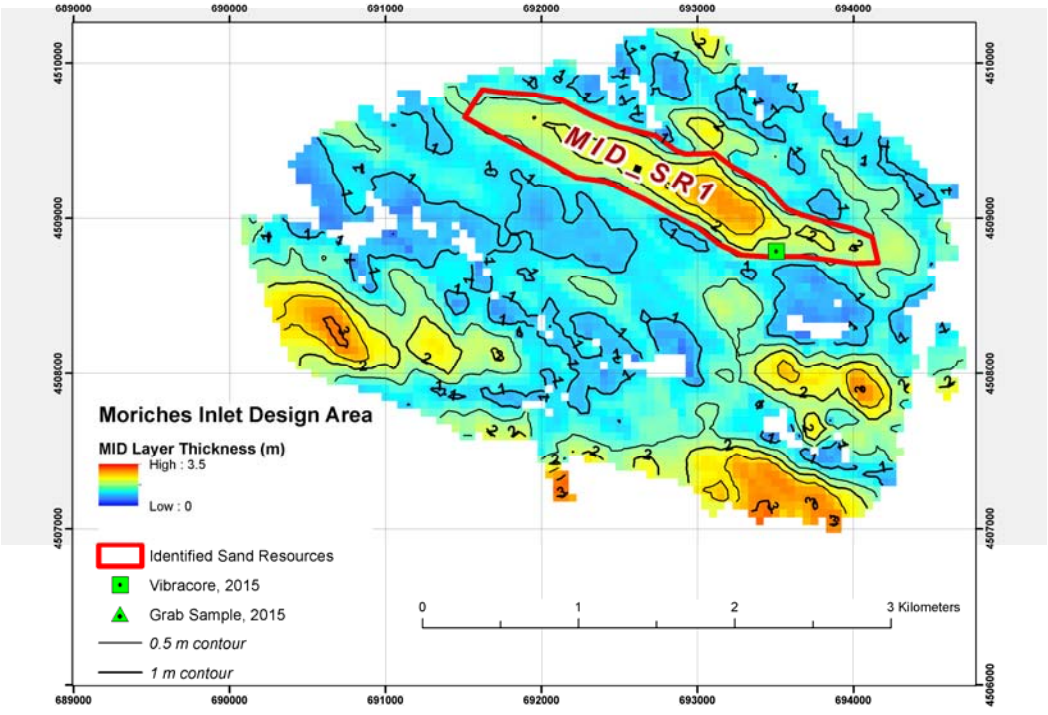


**Figure 31b. Potential and proven sand reserves identified at the Moriches Inlet site by identified by Flood et al. (2018).**

The estimated shoreline changes (recession) associated with the changes in the divergence in LST are shown in **Figures 32 - 34** for excavation of the entire borrow areas, and in **Figures 35 - 37** for the removal of only the potential and proven sand reserves**.** In these figures, the divergence in LST is converted to a rate of shoreline change using the engineering expedient: a change in divergence of one cubic yard per foot of shoreline corresponds to a change in one foot of beach width (Waldner, 2004). To interpret these figures, note the following:

- Values less than zero represent additional erosion: if the beach were eroding before the excavation, the erosion increases by the value indicated. If the beach is accreting before the excavation of the borrow area, the rate of accretion decreases by the value indicated.
- Values greater than zero represent accretion.
- Once these changes are effected by offshore sand mining in the borrow areas, they would be permanent, at least until the borrow area morphology is changed.
- Highly variable values at inlets far from the borrow-area locations are artificial artifacts due the rapid variation of shoreline direction around the inlets and should be ignored.

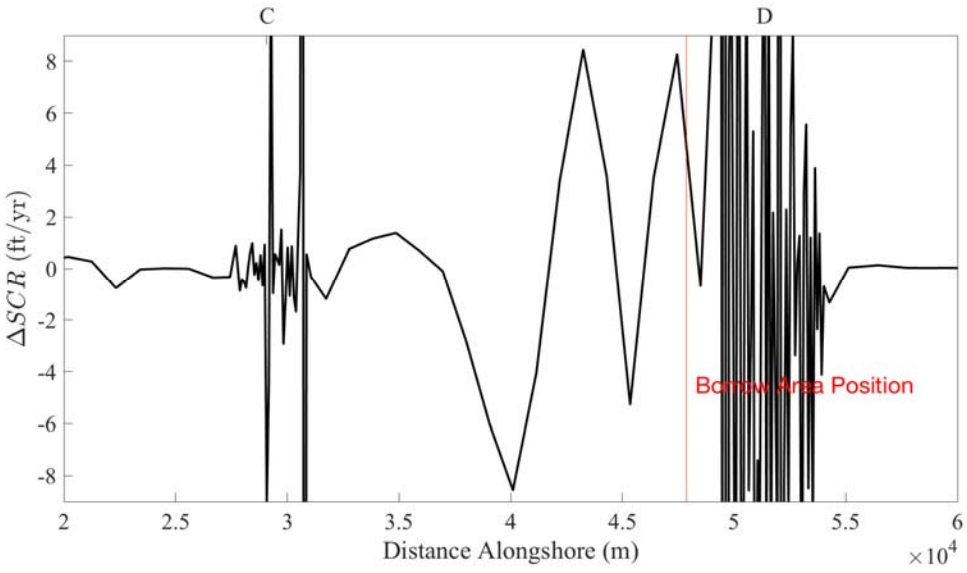


**Figure 32. The change in shoreline recession rate due to the excavation of the entire area associated with the FI Inlet borrow area to a depth of 4 meters.**

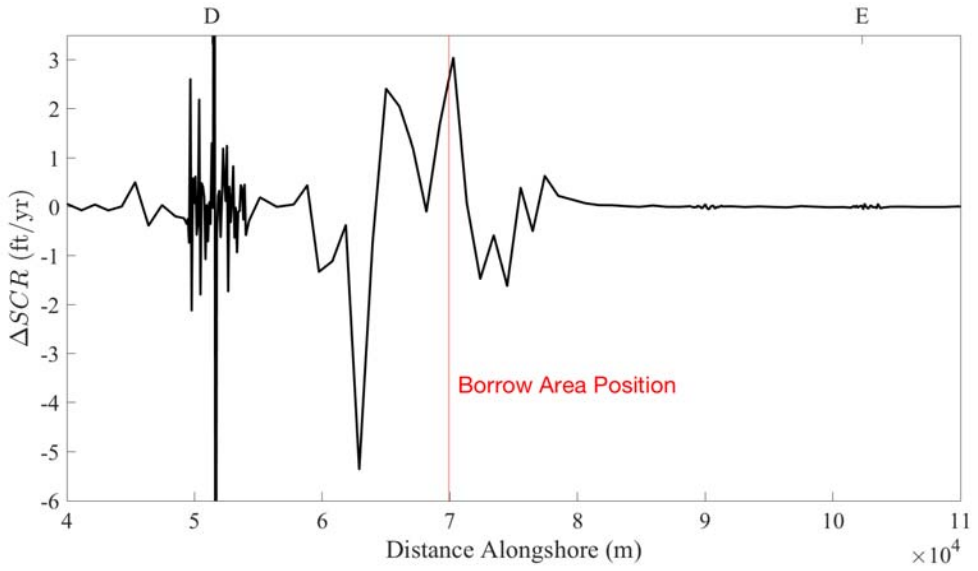


**Figure 33. The change in shoreline recession rate due to the excavation of the entire area associated with the FI borrow area to a depth of 4 meters.**

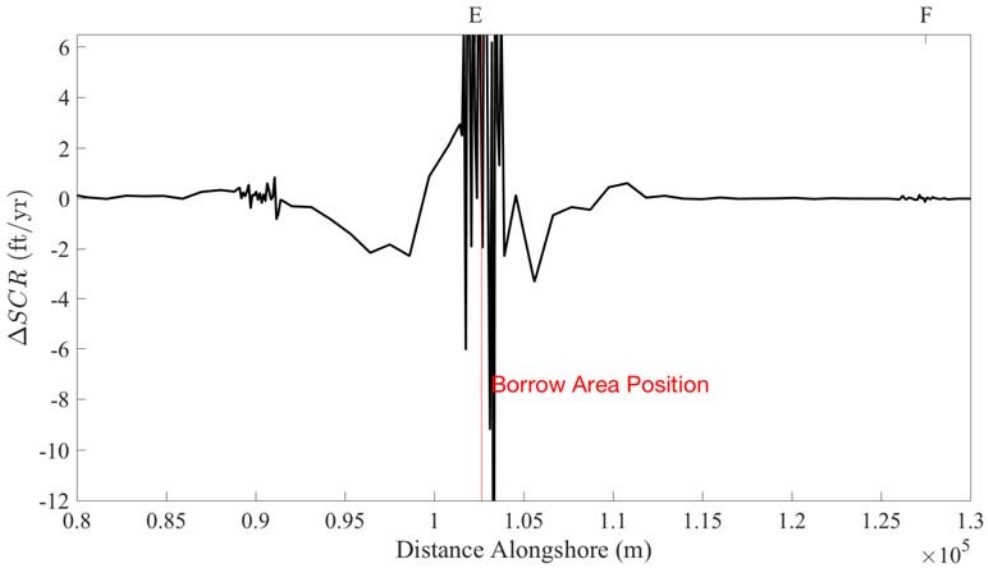


**Figure 34. The change in shoreline recession rate due to the excavation of the entire area associated with the Moriches Inlet borrow area to a depth of 4 meters.**

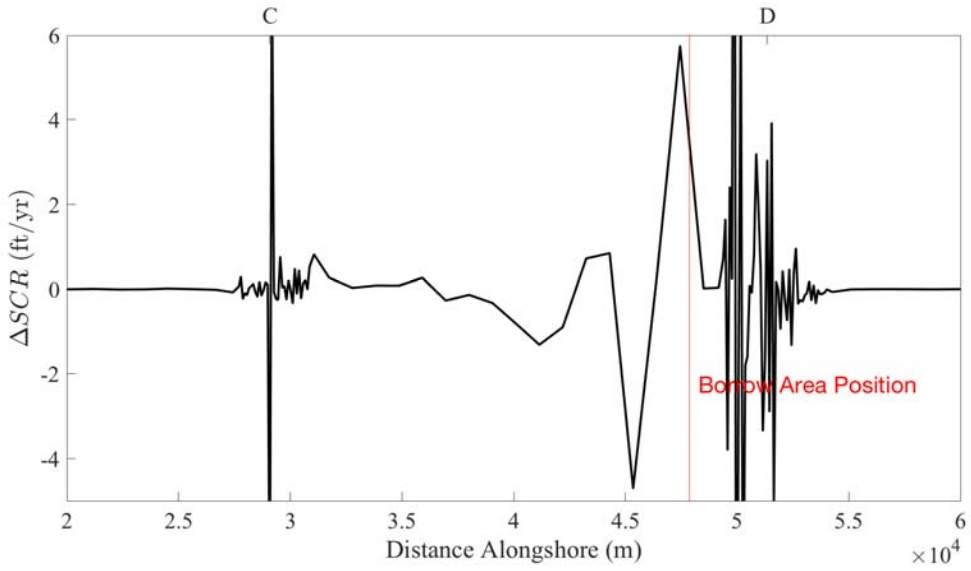


**Figure 35. The change in shoreline recession rate due to the excavation of potential sand reserves identified at the Fire Island Inlet site (Figure 29b).**

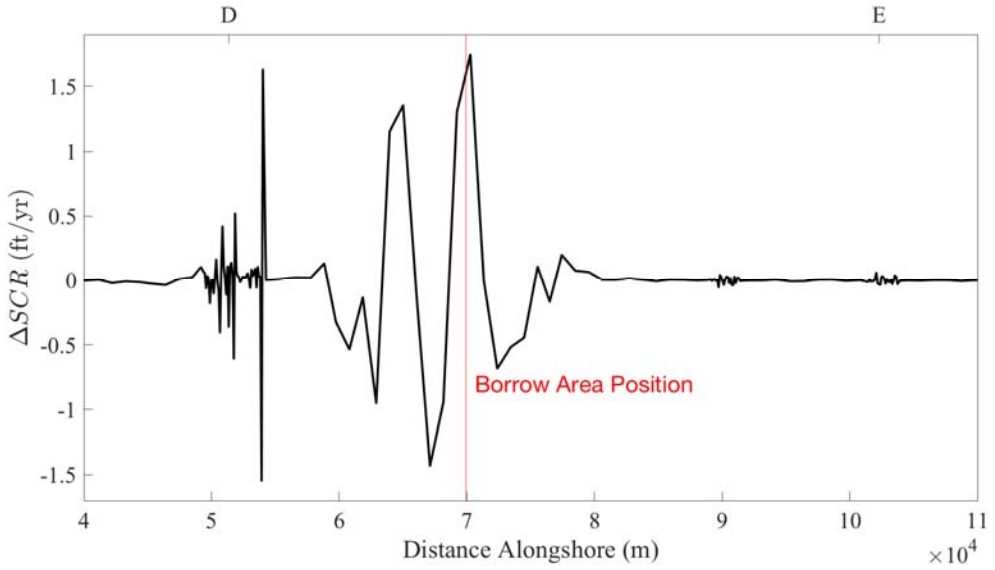


**Figure 36. The change in shoreline recession rate due to the excavation of potential sand reserves identified at the Fire Island site (Figure 30b).**

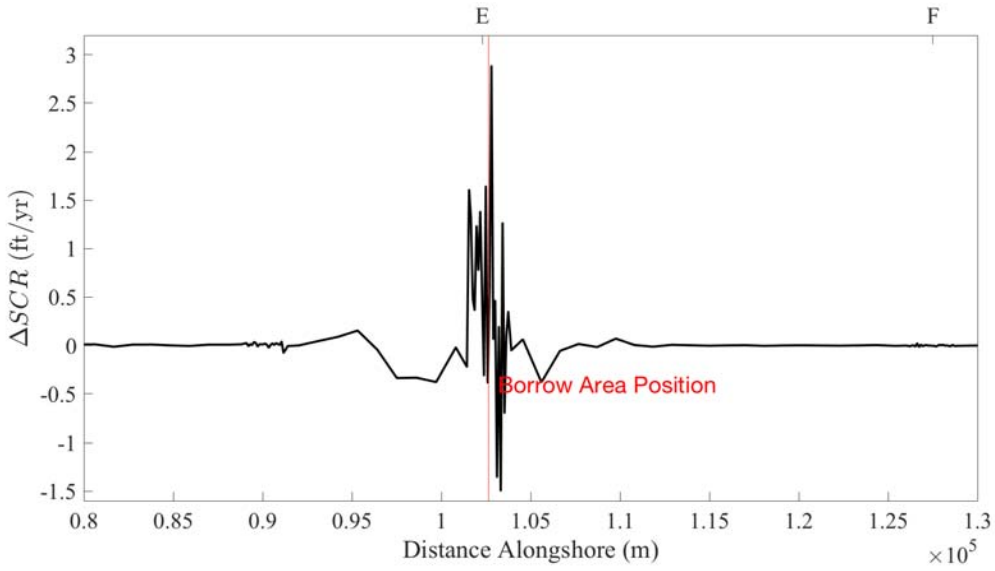


**Figure 37. The change in shoreline recession rate due to the excavation of potential sand reserves identified at the Moriches Inlet site (Figure 31b).**

## *References*

Benedet, L., Finkl, C.W., and Dobrochinski, J., 2013, Optimization of nearshore dredge pit design to reduce impacts on adjacent beaches: Journal of Coastal Research, v. 29, no. 3, p. 519–525.

Bokuniewicz, H, 2018. Personal Communication.

Dalyander, P.S., Mickey, R.C., Long, J.W., and Flocks, James, 2015. Effects of proposed sediment borrow pits on nearshore wave climate and longshore sediment transport rate along Breton Island, Louisiana: U.S. Geological Survey Open-File Report 2015–1055, 41 p., http://dx.doi.org/10.3133/ofr20151055.

Dean, R. G. and R. A. Dalrymple (2004). Coastal processes with engineering applications, Cambridge University Press.

Flood, R., J. Lashley, I. Dwyer and H. Bokuniewicz, 2018. Technical Report on G&G Data Analysis and Delineation of Potential Sand Borrow Areas, Report to NYS Department of State: 60 pp.

Kana, T.W. 1995. A mesoscale sediment budget for Long Island, New York. 1995, Marine Geology 126: 87-110.

Long, J.W., N.G. Plant, P.S. Dalyander, and D.M. Thompson, 2014. A probabilistic method for constructing wave time-series at inshore locations using model scenarios, Coastal Engineering 89: 53–62 doi:10.1016/j.coastaleng.2014.03.008.

Longuet-Higgins, M., 1952, On the statistical distribution of the height of sea waves: Journal of Marine Research, v. 11, p. 245–266.

Longuet-Higgins, M., 1972, Recent progress in the study of longshore currents, *in* Meyer, R.E., ed., Waves on beaches: New York, Academic Press, p. 203–248.

Rosati, J.D., M.B. Gravens and W.G. Smith, 1999. Regional sediment budget for Fire Island to Montauk Point, New York, USA, 4th International Symposium on Coastal Engineering and Science of Coastal Sediment Processes Coastal Sediments '99: 802-817.

van Rijn, L.C., 2014, A simple general expression for longshore transport of sand, gravel and shingle, Coastal Engineering 90:23–39.

Waldner, J., 2004. Sand resources for shore protection projects in New Jersey, New Jersey Geological Survey Information Circular: 2pp.

Wilson, R., A. Ilia, H. Bokuniewicz and C. Hinrichs, 2016. Technical report on physical wave modeling. Unpublished report to NYS DOS, School of Marine and Atmospheric Sciences, Stony Brook University: 11pp.